Observing the Position Spread of Atomic Wave Packets

A. Görlitz,[1] M. Weidemüller,[1,*] T. W. Hänsch,[1] and A. Hemmerich[2,†]
[1]*Sektion Physik, Universität München, Schellingstrasse 4/III, D-80799 München and Max-Planck-Institut für Quantenoptik, D-85748 Garching, Germany*
[2]*Institut für Laserphysik, Universität Hamburg, Jungiusstrasse 9, D-20355 Hamburg, Germany*
(Received 2 December 1996)

We report on a novel method to measure the spatial extension of atomic wave packets confined in the microscopic light traps of a three-dimensional optical lattice. We compare the powers Bragg scattered by two different classes of lattice planes from two blue light beams incident on the atomic lattice under different Bragg angles. We have used this technique to explore unusual atomic vibrational modes which display a position spread oscillating at twice the fundamental vibrational frequency. [S0031-9007(97)02581-7]

PACS numbers: 42.50.Gy, 32.80.Pj, 42.50.Vk, 42.62.Fi

Refined laser cooling and trapping techniques have recently led to a novel type of cold matter: three-dimensional lattices of ultracold atoms bound by standing light waves in microscopic traps operating in the Lamb-Dicke regime [1]. Very recently Bragg diffraction, a method well known from crystallography, has been successfully applied to such "optical lattices" and hopes were raised that this could prove to be a powerful tool to investigate novel aspects of these highly ordered cold atomic samples [2,3]. In this Letter we report on a method to measure the position spread of atoms trapped in the potential wells of an optical lattice. We exploit the fact that the cross section for Bragg diffraction scales with the Debye-Waller factor which exponentially depends on the atomic position spread measured in units of the distance between adjacent lattice planes. By comparing the powers diffracted into Bragg maxima arising from two different sets of lattice planes we can directly measure the atomic position spread. This technique offers unique reliability because it does not require any information on the atomic species (atomic polarizability, atomic density) or on the peculiarities of the cooling and trapping mechanism (cooling rate, etc.). It should work for "bright" and "dark" optical lattices operating near or far off resonance. Potential applications can be envisioned, e.g., in atomic lithography experiments where a simple and reliable online method to observe the degree of atomic localization is desired [4].

Our new diagnostic tool opens intriguing possibilities to study the vibrational dynamics of trapped atoms. As one example we have explored unusual vibrational modes characterized by an oscillating atomic position spread. Such breathing modes can be excited by a rapid nonadiabatic change of the trapping potential depth which is readily achieved by adjustment of the light power of the trapping beams. The atomic wave function cannot instantaneously adjust itself to the altered potential well resulting in cycles of compression and expansion at twice the fundamental vibrational frequency [5]. In principle, this should allow one to prepare atomic samples which are localized beyond the position spread of the vibrational ground state, which would correspond to "squeezing" in a mechanical harmonic oscillator [6]. In practice, various mechanisms can counteract position spread oscillations. Optical pumping leads to a pure decay of this oscillation involving different time constants characteristic for the dynamics of Sisyphus cooling [7]. Anharmonicity of the potential wells can disperse the oscillating wave packets because different parts of the wave packets oscillate with slightly different frequencies. This typically yields a second source of decay of the breathing oscillation; however, under certain circumstances, a rephasing may occur leading to subsequent revivals.

Our experimental setup for Bragg diffraction builds on that described in Ref. [2]. The optical lattice is loaded by means of a magneto-optic trap (MOT) which collects rubidium atoms from a hot dilute vapor at room temperature. After typically 100 ms of gathering atoms the MOT is turned off and the atoms are released into the optical lattice. The body-centered cubic (bcc) lattice [8] is formed within a few hundred microseconds by three mutually orthogonal optical standing waves at $\lambda_r = 780$ nm tuned to the red side of the $5S_{1/2}(F = 3) \rightarrow 5P_{3/2}(F' = 4)$ transition of ^{85}Rb. We have taken care in adjusting the power ratios for the three standing waves such that the potential wells at each lattice site are isotropic at their bottom. For Bragg diffraction we use blue light tuned near to the $5S_{1/2}(F = 3) \rightarrow 6P_{1/2}(F' = 2$ or $F' = 3)$ transition at $\lambda_b = 421.7$ nm in order to enhance the scattering cross section. We use only a few ten microwatts in collimated beams of 5 mm diameter in order to avoid large radiation pressure on the trapped atoms. The bandwidth of this light is adjusted to approximately 10 MHz in order to exceed the inhomogeneous broadening from light shifts experienced by the trapped atoms. Two such blue beams are incident on the lattice satisfying the Bragg condition for Bragg angles $\theta_1 = 57.3°$ and $\theta_2 = 31.4°$ to better than 0.1 mrad with respect to two different classes of lattice planes, i.e., the [1,0,0] and the [3,1,0] planes if the bcc lattice is described by a biatomic Cartesian unit cell.

 0031-9007/97/78(11)/2096(4)$10.00

This is indicated in Fig. 1(a) where the bcc lattice is projected onto the *xy* plane with unfilled and filled circles representing the two classes of atoms forming the biatomic unit cell. When the Bragg condition is met in either of the beams we observe a strong increase of the scattered power by at least 3 orders of magnitude as compared to the background of diffuse scattering (no cross talk between the two beams is observed). Our setup for Bragg scattering works only for three dimensions. If we block the lattice beams along the *z* axis, we can switch from the spin-polarized bcc lattice to a two-dimensional configuration where two face-centered square lattices with trapping sites for atoms of antiparallel angular momenta are interleaved. This gives rise to additional lattice planes for the [3,1] direction. Hence destructive interference arises and thus we do not observe a Bragg maximum for the [3,1] direction in this case.

For isotropic potential wells we can relate the powers P_1 and P_2 diffracted from the two blue probe beams to e.g., the *y* component of the position spread

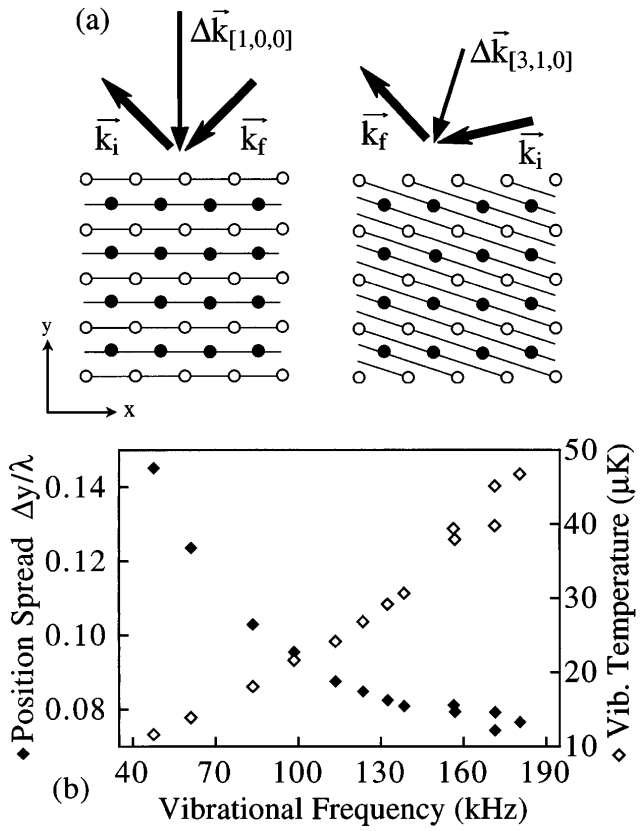

FIG. 1. (a) Two blue (421 nm) laser beams are Bragg scattered by the [1,0,0] (left detail) and the [3,1,0] lattice planes of an optical lattice operating with near infrared light at 780 nm. The power scattered by each beam is measured and the atomic position spread is obtained by means of Eq. (1). (b) Atomic position spread (filled marks) along the normal on the [1,0,0] planes and corresponding vibrational temperature (unfilled marks) plotted versus the fundamental vibrational frequency in the potential wells.

$$\Delta y^2 = \frac{\lambda_r^2}{24\pi^2}[\ln(P_1) - \ln(P_2)]. \quad (1)$$

Let us briefly discuss the assumptions at the basis of this equation. Consider a density operator ρ describing the spatial distribution of an atom trapped at some lattice site. The coherent scattering cross section scales with an attenuation factor $\langle \exp(i\Sigma\Delta k_l R_l)\rangle$ where Δk_l are Cartesian components of the difference between the incident and the diffracted wave vectors, R_l are the corresponding components of the position operator, and the brackets indicate the expectation value with respect to ρ (Σ = sum over $l = x, y, z$) [9]. If ρ satisfies the condition $\langle R_l^{2n}\rangle = 1 \times 3 \times \cdots \times (2n-1)\,\langle R_l^2\rangle^n$ the attenuation factor becomes the well known Debye-Waller factor $\exp(-2W)$ where $2W$ equals $\Sigma\Delta k_l^2 \Delta R_l^2$ and Eq. (1) follows immediately by assuming an isotropic potential. We may, e.g., adopt a harmonic oscillator model to describe the low lying vibrational levels which seems well justified for potential wells exceeding a few hundred recoil energies [5]. In this case the position distribution of a thermal atomic sample ρ has a Gaussian shape and the above relation between $\langle R_l^{2n}\rangle$ and $\langle R_l^2\rangle^n$ holds. However, we should keep in mind that Eq. (1) is slightly more general.

In Fig. 1(b) we show a measurement of the atomic position spread (filled marks) versus the fundamental vibrational frequency which was varied by changing the intensity of the lattice beams. The values for the fundamental vibrational frequencies were directly measured by means of stimulated Raman spectra [10] and alternatively by evaluation of the potential depth as calculated from the antinode Rabi frequency and the frequency detuning of the lattice. Both results agree to better than 5%. At the highest vibrational frequencies which we could adjust we find values of Δy down to a 13th of the optical wavelength of 780 nm. Remarkably, Δy decreases up to larger values of the potential depth than predicted by one-dimensional calculations [5] while the corresponding vibrational temperature (unfilled marks) (which is readily calculated from Δy in the harmonic approximation) increases from left to right in Fig. 1(b) as expected.

We now turn to the observation of atomic wave packets with oscillating position spread. Our starting point is a thermal atomic state in a potential $U(\omega_i)$ characterized by the fundamental vibrational frequency ω_i. We then switch nonadiabatically (i.e., satisfying the relation $\partial\omega/\partial t > \omega^2$) to a steeper potential with vibrational frequency $\omega_f > \omega_i$. The initial atomic density distribution cannot instantaneously adjust to the increasing steepness of the potential wells and thus excess potential energy is applied to the wings of the initial atomic density distribution as compared to the case of adiabatic compression. This leads to an oscillation of the position spread Δy of the atomic wave packet at twice the final vibrational frequency ω_f. In terms of quantum mechanics the oscillation of Δy results from the buildup of coherences between vibrational

levels $|n\rangle$ and $|n + 2\rangle$ with vibrational quantum numbers which differ by two. More specifically, since $\langle y\rangle = 0$ we can express Δy^2 as

$$\Delta y^2 = \frac{\lambda_r^2}{4\pi^2}\frac{\omega_{\rm rec}}{\omega_f}\sum_{n=0}\sqrt{(n+1)(n+2)} \times (\rho_{nn+2} + \rho^*_{nn+2}) + (2n+1)\rho_{nn}\,. \quad (2)$$

Here $\omega_{\rm rec}$ is the recoil energy of a single photon divided by Planck's constant. The first class of terms in the sum in Eq. (2) involves coherences ρ_{nn+2} between levels $|n\rangle$ and $|n + 2\rangle$. The time evolution of these terms is given by complex phase factors oscillating at frequencies $2(\omega_f - \delta_n)$ where δ_n represent small (positive) corrections which increase with growing n and which describe the anharmonicity of the potential wells. The series of growing values of δ_n leads to a dephasing and under certain circumstances to a subsequent rephasing of the coherences. The characteristic dephasing time is on the order of $2\pi/\Delta$ where Δ represents an upper bound of those δ_n's corresponding to significantly populated states $|n\rangle$. If the n dependence of the δ_n's is not too different from the linear case, complete rephasing occurs after a typical time on the order of $2\pi/\delta$ where δ denotes an average value for $\delta_{n+1} - \delta_n$. Partial rephasing, however, may occur at earlier times. We may summarize that the ρ_{nn+2} terms in Eq. (2) describe the breathing motion of the atomic wave packet around a mean value given by the second part of the sum which involves the time-independent populations ρ_{nn}.

In the previous discussion we have so far neglected dissipation. Assuming that the buildup of coherences only occurs during switching we may model the relaxation of the coherences ρ_{nn+2} as a pure decay process [in contrast to the more complex relaxation of the populations which are subject to the condition $\mathrm{Tr}(\rho) = 1$, because no loss of atoms can occur within the typical relaxation time]. In optical lattices Raman transitions between vibrational levels lead to relaxation of the vibrational levels at rates approximately given by $\gamma_n = (2n + 1)\,\gamma$, where the ground state relaxation rate γ equals the optical pumping rate Γ' for an unbound atom multiplied with the small Lamb-Dicke factor $\omega_{\rm rec}/\omega_f$ [10]. In case of equidistant vibrational levels (as found in a harmonic potential) this does, however, not yield a decay of coherences ρ_{nm} because the spontaneous photons arising in the Raman processes connecting the states $|n\rangle \rightarrow |n + k\rangle$ and $|m\rangle \rightarrow |m + k\rangle$ cannot be distinguished. If, however, the anharmonic corrections δ_n become comparable with γ_n, such photons can be discriminated in terms of frequency. In this case each spontaneous Raman process is connected with a partial decay of coherence, i.e., after a few such processes coherence will be completely lost. According to these considerations we expect the dissipative decay rate for the position spread oscillations to be typically several times smaller than γ, i.e., on the order of a few $10^4\ \mathrm{s}^{-1}$. This is the reason why we may expect a revival to occur within the dissipative decay time. Note that in accordance with our expectations, quantum-Monte-Carlo calculations by researchers at NIST indicate that, in fact, coherence is preserved over a few times $1/\gamma$ [11]. The time scale for the relaxation of the populations towards their steady state values in the compressed potential is determined by the rates for spontaneous Raman transition which change the magnetic quantum number and which are responsible for Sisyphus cooling [12]. Such processes occur at rates which can be significantly smaller than γ (owing to small Clebsch-Gordan coefficients) and, consequently, cooling (heating) rates in optical lattices can be below $10^4\ \mathrm{s}^{-1}$.

A typical observation is shown in Fig. 2. After the potential well is raised within 500 ns at $t = 16\ \mu$s from

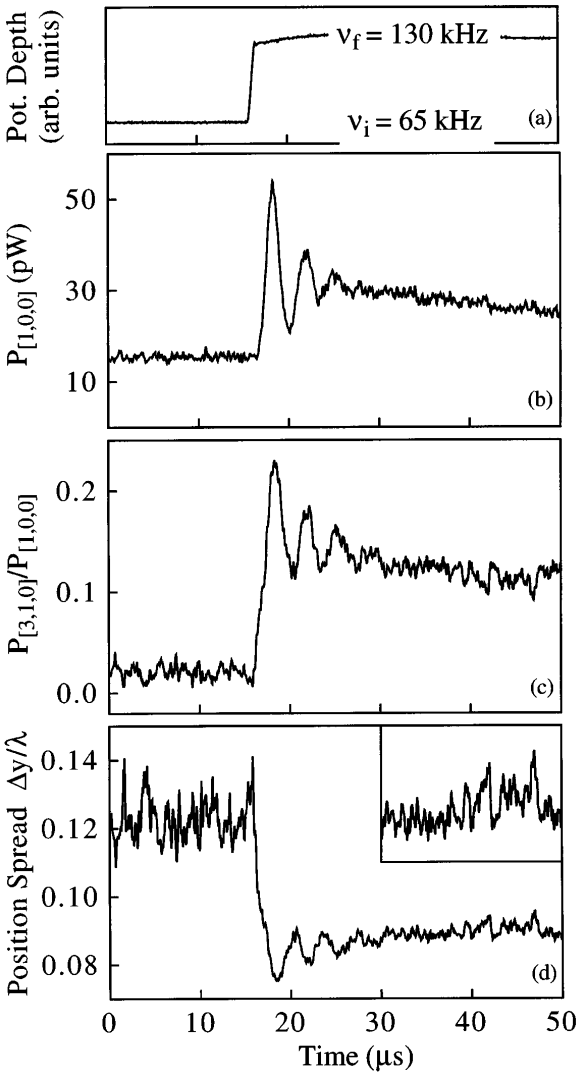

FIG. 2. (a) The potential well initially characterized by the fundamental vibrational frequency $\nu_i = 65$ kHz is raised at $t = 16\ \mu$s within 500 ns to $\nu_f = 130$ kHz. (b) Power of 421 nm radiation scattered from the [1,0,0] lattice planes plotted versus time. (c) Power ratio $P_{[3,1,0]}/P_{[1,0,0]}$ plotted versus time. (d) Atomic position spread calculated from (c) by means of Eq. (1).

$\omega_i/2\pi = 65$ kHz to $\omega_i/2\pi = 130$ kHz [Fig. 2(a)] we see for both Bragg beams a sudden increase of the diffracted power followed by a rapid oscillation which decays in about 10 μs. In Fig. 2(b) this is shown for the power $P_{[1,0,0]}$ scattered from the [1,0,0] planes. We typically recognize four maxima of this oscillation. We have checked that the observed oscillation frequency approximately equals $2\omega_f$ by extracting the value of ω_f from a probe transmission spectrum. A second much slower decay is also observed (with a time constant of typically several ten μs) which we attribute to the relaxation of the vibrational populations arising because the equilibrium temperature in the new potential approached by Sisyphus cooling can differ from the temperature reached by pure adiabatic compression. Note that a change of the atomic position spread is accompanied by a change of the single atom scattering cross section, because the resonance condition for the blue probe beams depends on the power broadening introduced by the infrared lattice beams. Therefore recording a single Bragg maximum as in Fig. 2(b) is not a sufficient means to study oscillations of the atomic position spread.

In Fig. 2(c) we show the ratio between the powers $P_{[3,1,0]}$ and $P_{[1,0,0]}$ scattered from the [3,1,0] and the [1,0,0] planes and in Fig. 2(d) the corresponding position spread is plotted as calculated from the graph in Fig. 2(c) according to Eq. (1). In the region between $t = 35$ μs and $t = 50$ μs of trace Fig. 2(d) [and Fig. 2(c) as well] we recognize additional structure rising out of the noise. This section of the spectrum is shown with expanded abscissa in the upper right corner of Fig. 2(d). Although this structure is readily reproduced and certainly does not represent an artifact, its small size prevents a thorough analysis of its physical origin. However, according to our previous discussion it is conceivable that the observed structure originates from rephasing of the coherences before they decay by dissipation. The physical significance of the observed revival is emphasized by the fact that it occurs in both powers $P_{[3,1,0]}$ and $P_{[1,0,0]}$ independently. For $P_{[1,0,0]}$ it is smaller in accordance with the fact that this signal is less sensitive to the atomic position spread. In our experiments we took care to produce isotropic potential wells by carefully adjusting the powers of the lattice beams, the light polarizations, and the time-phase differences. Improper adjustment of these parameters introduces anisotropy which is particularly disturbing in the $P_{[3,1,0]}$ signal because it measures the position spread along the $(\mathbf{e}_x + 3\mathbf{e}_y)$ direction while $P_{[1,0,0]}$ is solely sensitive to the $\mathbf{e}_y$ direction. Experimentally, we in fact find $P_{[3,1,0]}$ to oscillate at different frequencies in this case.

In summary, we have presented a new experimental method to obtain direct information on the position spread of atoms trapped in steep microscopic potential wells in an optical lattice. Our method is remarkably reliable because it does not rely on any inaccurately known system parameters. We have used this technique to identify atomic wave packets with a position spread oscillating in time at twice the fundamental vibrational frequency. We have observed a decay and possibly a revival of these oscillations on a time scale of several ten microseconds and interpreted them in terms of dephasing and rephasing effects connected with the anharmonicity of the potential wells and dissipation due to optical pumping. We believe that our novel observation technique offers an attractive combination of simplicity and reliability and thus promises future applications, for example, in atomic beam lithography.

Part of this work has been supported by the German BMBF under Contract No. 13N6637/5. A. H. acknowledges invaluable discussions with C. Zimmermann.

Note added.—We have learned recently that related experimental work in a cesium optical lattice is under way at NIST [11] and a paper which reports it is now accepted for publication in Physical Review Letters.

*Present address: FOM Institut for Atomic and Molecular Physics, Kruislaan 407, 1098 SJ Amsterdam, The Netherlands.

†Electronic address: hemmerich@physnet.uni-hamburg.de

[1] A review of early experimental work is given in M. G. Prentiss, Science **260**, 1078 (1993); G. P. Collins, Phys. Today **46**, No. 6, 17 (1993). More recent work is reviewed in Ref. [8].

[2] M. Weidemüller *et al.*, Phys. Rev. Lett. **75**, 4583 (1995).

[3] G. Birkl *et al.*, Phys. Rev. Lett. **75**, 2823 (1995).

[4] G. Timp *et al.*, Phys. Rev. Lett. **69**, 1636 (1992); J. McClelland *et al.*, Science **262**, 877 (1993).

[5] S. Marksteiner *et al.*, Appl. Phys. B **60**, 145 (1995).

[6] D. M. Meekhof *et al.*, Phys. Rev. Lett. **76**, 1796 (1996).

[7] J. Dalibard and C. Cohen-Tannoudji, J. Opt. Soc. Am. B **6**, 2023 (1989).

[8] A. Hemmerich *et al.*, in *Proceedings of the International School of Physics "Enrico Fermi," Course CXXXI, 1995, Varenna, Italy*, edited by R. Bonifacio, W. Barletta, and A. Aspect (North-Holland, Amsterdam, 1996).

[9] N. Ashcroft and N. D. Mermin, *Solid State Physics* (Holt-Saunders, Tokyo, 1981).

[10] J. Courtois and G. Grynberg, Phys. Rev. A **46**, 7060 (1992).

[11] G. Raithel (private communication).

[12] J. Dalibard and C. Cohen-Tannoudji, J. Opt. Soc. Am. B **6**, 2023 (1989).